Benin-Irrua Transmission Line Voltage Stability Condition: Evaluating the Stability Indices

Peter Michael ENYONG[1] and Abdulai Braimah OSHOMAH[2]

[1,2]*Department of Electrical/Electronic Engineering Technology, Auchi Polytechnic, Auchi, Nigeria*
pmenyong@yahoo.com / abdulaioshomah@yahoo.com

Corresponding Author: pmenyong@yahoo.com

Date Submitted: 08/02/2019
Date Accepted: 23/03/2019
Date Published: 30/04/2019

***Abstract**: The voltage stability condition of the Benin-Irrua 132 KV medium transmission line (MTL) was investigated. This paper presents the approaches to the evaluation of ten relevant stability indices to that effect. Six stability indices by load-and-system impedance method include Voltage Stability Load Bus Index (VSLBI), Impedance Stability Index (ISI), Fast Voltage Stability Index (FVSI), Voltage Index Predictor (VIP), Transmission Path Stability Index (TPSI) and Line Stability Index (Lmn). The other four indices evaluated by the maximum-loadability method were Voltage Stability Index (VSI), Power Transfer Stability Index (PTSI), Voltage Collapse Potential Indices (VCPI's), and Voltage Stability Margin (VSM). In tandem with their various standard specifications (in per unit terms): only two of the ten indices, VSI(0.45) and TPSI(0.47), gave indications close to a 50/50% chance of stable and collapsed conditions; which is considered okay. The indices FVSI(0.11), Lmn(0.12), PTSI(0.23), VCPI(0.23) and VSM(0.76), five of them provided indications to very good voltage stability condition; whereas, the remaining three, ISI(0.07), VIP(1.00) and VSLBI(29.67), constituted pointers to excellent static voltage stability condition. Thus, the line was adjudged to be in good voltage stability condition.*

***Keywords:** Medium transmission line, Network voltage condition, Survey of stability indices, Load flow analysis, MATLAB.*

1. INTRODUCTION

The Benin-Irrua 132 KV transmission line in Nigeria is a medium transmission line (MTL), being of length which falls within the 80 to 250 km range often stipulated for such categories of power lines, other factors notwithstanding [1, 2]. For reasons of system planning, and effective and efficient operation, it became necessary to survey the voltage stability of the line, more so in the face of the growing heaviness of our national maximum demand.

Generally, power system stability may be defined as that property of a power system that enables it to remain in a state of operational equilibrium under normal working conditions, and to regain an acceptable state of equilibrium after being subjected to disturbance or disturbances [3]. Voltage stability is defined as the ability of a power system to maintain acceptable voltage at all buses under normal operating conditions and after subjection to a given disturbance or disturbances [3, 4].

As a power system becomes complex and heavily loaded, alongside economic and environmental constraints, the sustainability of voltage stability becomes an issue requiring serious consideration. This is because such conditions will usually lead to the power system being operated close to its stability limits [5], meaning a sure invitation of voltage instability and/or frequency instability, as the case may warrant; whether static or dynamic in dimension. Obviously, voltage stability is one of the major categories of power system stability (see Classification in Fig. 1). Absence of this property of a power system, or precisely a transmission line in this case, often brings about an uncontrollable drop (or rise) in the system voltages when a disturbance takes place. It will always begin as a local occurrence, before the effects escalate and may swallow a larger area of the power system due to the cascading effects; and it would then be referred to as a voltage collapse having occurred [6].

 ISSN: 2645-2685

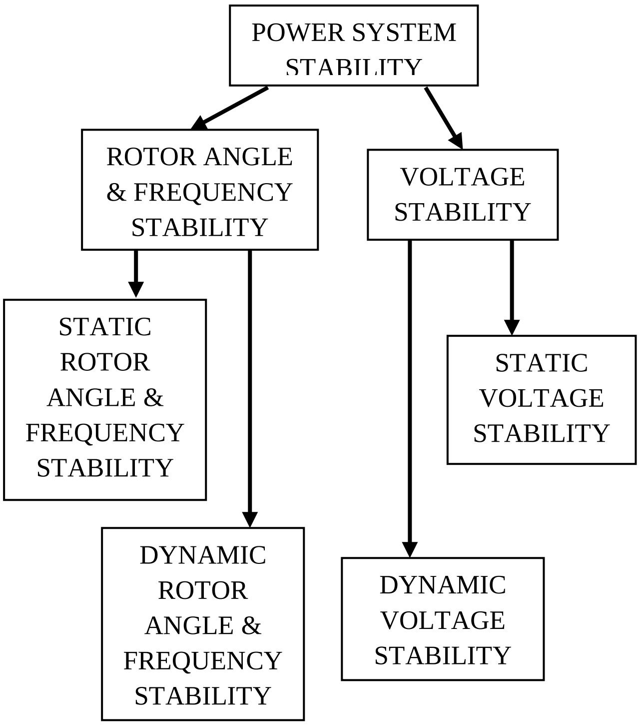

Fig. 1: A Broad Classification of Power System Stability

Essentially, it is inadequate reactive power resource that is at the root of every instance of voltage collapse [7]. Indeed, voltage collapse is no other phenomenon than that extreme level of voltage instability caused by gross inability of the power system to supply the reactive power adequate to sustain the original and acceptable voltage profile, or by excessive absorption of reactive power by the system itself [8, 9]. Therefore, more often than not, the central objective of voltage stability analysis is to find out the weak areas of the system in terms of reactive power deficiency, and determine the critical emergences and voltage stability margins, for various amounts of power transfer within areas of the system. Of course, this is the core objective of this research work hereby presented to the reading society.

2. METHODOLOGY

Before the description of the methods adopted for the realization of the objectives of this work, it is important to dwell though succinctly on the composition and representation of the line in question; as part of the materials for use in this work.

2.1 Salient Constituent Parts of the Line and Its Representation

From field work realizations, the Benin-Irrua 132 KV transmission line system is made up of a total series impedance of $0.2105\angle 74.1^{o}$ (p.u.); a total shunt admittance of $0.03764\angle 90^{o}$ (p.u.); conductors of 360 mm^2, and length of 81 km. And the line supplies a complex peak load demand of $0.34\angle 22.5^{o}$ (p.u.), on the average [10]. It is represented as in Fig.2 taking a cue from [11] and its operational base voltage of 132 KV falls within the 100 – 138 KV range associated with medium lines [12]. Hence, it is referred to as a medium transmission line (MTL).

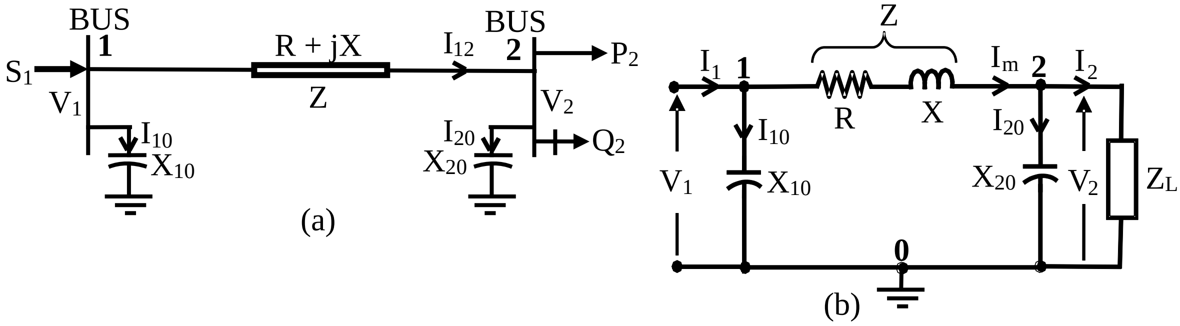

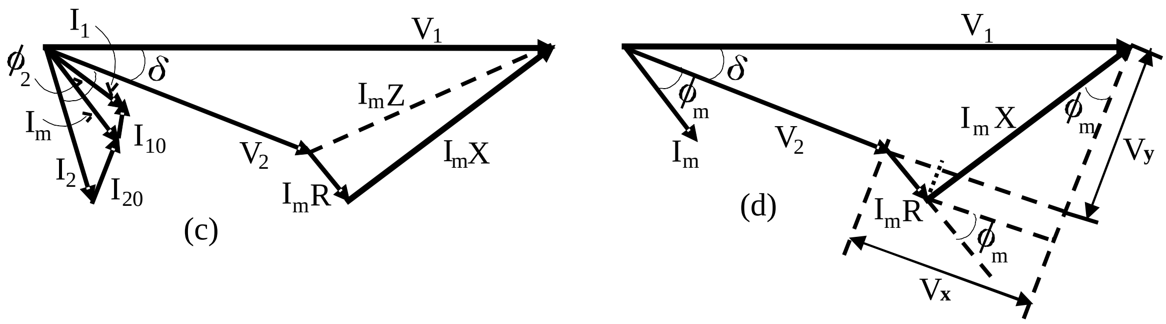

Fig. 2: (a) One-Line Diagram of the MTL; (b) Nominal-Π Equivalent Circuit of the MTL; (c) Phasor Diagram relative to the Equivalent Circuit; (d) Short-Line Equivalent of the Nominal-Π Equivalent Circuit Phasor Diagram

It is important to state that the nominal-π equivalent circuit is preferred here to the other forms of representation because of the advantage of making use of the associated short-line equivalent circuit of the MTL [13]. Of course, as given in Fig. 2(d), this is only realizable from the nominal-π equivalent circuit. In the phasor diagrams, it will be seen that the input-end voltage is made the reference vector; whilst the output-end voltage lags it by a given angle [6, 11, 14]. It might be necessary at this juncture to present the following definition of parameters with values (where stipulated) as earlier given in [10] concerning the line:

$V_1 = |V_1|\underline{/0^o}$; $V_2 = |V_2|\underline{/\delta}$ (input-end and output-end voltages, respectively; δ, being the transmission angle)
$I_1 = |I_1|\underline{/\phi_1}$; $I_m = |I_m|\underline{/\phi_m} = I_{12}$; $I_2 = |I_2|\underline{/\phi_2}$ (input, mid-span and output currents, respectively)
$I_{10} = |I_{10}|\underline{/\phi_{10}}$; $I_{20} = |I_{20}|\underline{/\phi_{20}}$ (input-end and output-end line-charging currents, respectively)
$Z = R + jX = [7.598 + j20.62]\ \Omega$ (line impedance, resistance (R) and inductive reactance (X))
$X_{10} = X_{20} = -j0.926$ or $0.926\underline{/-90^o}$ kΩ (input-end and output-end line-to-ground or shunt capacitive reactances, respectively)
S_1; $S_2 = P_2 + jQ_2$ (input complex power; output complex power; active power (P_2=31.4 MW) and reactive power (Q_2=13.0 MVAr), respectively)
$Z_L = |V_2|^2/S_2^*$ (load impedance)
$(MVA)_{base} = 100$; $(KV)_{base} = 132$; (line base power and voltage, respectively)
$Z_{base} = |(KV)^2_{base}|/(MVA)_{base} = 174.24\ \Omega$; (line base impedance)

2.2 The Methods Adopted

Load-flow analysis with Newton-Raphson algorithm was particularly used in the determination of the Irrua (Load Bus) voltage and angle, V_2 and δ_2, respectively. Also, load-flow equations were used to obtain the maximum power deliverable (P_{2max}) and the line maximum reactive power capability (Q_{2max}). Details of the load-flow equations as in [10] are provided here as follows:

$$P_2 = |V_2||V_1||Y_{21}|[\cos(\theta_{21}+\delta_1)\cos\delta_2 + \sin(\theta_{21}+\delta_1)\sin\delta_2] + |V_2|^2|Y_{22}|\cos\theta_{22}; \quad (1)$$

$$Q_2 = -|V_2||V_1||Y_{21}|[\sin(\theta_{21}+\delta_1)\cos\delta_2 - \cos(\theta_{21}+\delta_1)\sin\delta_2] - |V_2|^2|Y_{22}|\sin\theta_{22}; \quad (2)$$

Equations (1) and (2) are linearized by application of the Jacobian matrix:

$$J = \begin{bmatrix} J_{11} & J_{12} \\ J_{21} & J_{22} \end{bmatrix} \quad \text{(Jacobian matrix)} \quad (3)$$

where

$$J_{11} = \partial P_2/\partial\delta_2;\ J_{12} = \partial P_2/\partial|V_2|;\ J_{21} = \partial Q_2/\partial\delta_2;\ J_{22} = \partial P_2/\partial|V_2| \quad (4)$$

The partial differentiations and their simplification will yield

$$J_{11} = |V_2||V_1||Y_{21}|\sin[(\theta_{21}+\delta_1) - \delta_2]; \quad (5)$$

$$J_{12} = |V_1||Y_{21}|\cos[(\theta_{21}+\delta_1) - \delta_2] + 2|V_2||Y_{22}|\cos\theta_{22}; \quad (6)$$

$$J_{21} = |V_2||V_1||Y_{21}|\cos[(\theta_{21}+\delta_1) - \delta_2]; \quad (7)$$

$$J_{22} = -|V_1||Y_{21}|\sin[(\theta_{21}+\delta_1) - \delta_2] - 2|V_2||Y_{22}|\sin\theta_{22}; \quad (8)$$

And the linearized equations are reflected in the matrices that follow

$$\begin{bmatrix} \Delta P_2 \\ \Delta Q_2 \end{bmatrix} = \begin{bmatrix} J_{11} & J_{12} \\ J_{21} & J_{22} \end{bmatrix} \begin{bmatrix} \Delta\delta_2 \\ \Delta|V_2| \end{bmatrix} \quad \text{and} \quad \begin{bmatrix} \Delta\delta_2 \\ \Delta|V_2| \end{bmatrix} = \begin{bmatrix} J_{11} & J_{12} \\ J_{21} & J_{22} \end{bmatrix}^{-1} x \begin{bmatrix} \Delta P_2 \\ \Delta Q_2 \end{bmatrix} \quad (9)$$

where

ΔP_2, ΔQ_2, $\Delta\delta_2$, $\Delta|V|_2$ are computed changes in P_2, Q_2, δ_2 and $|V_2|$

For iteration purposes, it can be written

$$P_2^{(k)} = |V_2|^{(k)}|V_1||Y_{21}|\cos[(\theta_{21}+\delta_1) - \delta_2^{(k)}] + [|V_2|^2]^{(k)}|Y_{22}|\cos\theta_{22}; \quad (10)$$

$$Q_2^{(k)} = -|V_2|^{(k)}|V_1||Y_{21}|\sin[(\theta_{21}+\delta_1) - \delta_2^{(k)}] - [|V_2|^2]^{(k)}|Y_{22}|\sin\theta_{22}; \quad (11)$$

where $P_2^{(k)}$ and $Q_2^{(k)}$ are values of P_2 and Q_2, from eqn.(1) and (2) for the k^{th} iteration process; k = 0, 1, … (being the indication of the iteration number undertaken).

$\Delta P_2^{(k)} = P_2^{(sch)} - P_2^{(k)}$; (change in P_2 during the k^{th} iteration) (12)

$\Delta Q_2^{(k)} = Q_2^{(sch)} - Q_2^{(k)}$; (change in Q_2 during the k^{th} iteration) (13)

$$J^{(k)} = \begin{bmatrix} J_{11}^{(k)} & J_{12}^{(k)} \\ J_{21}^{(k)} & J_{22}^{(k)} \end{bmatrix}; \qquad inv\{J^{(k)}\} = inv\left\{\begin{bmatrix} J_{11}^{(k)} & J_{12}^{(k)} \\ J_{21}^{(k)} & J_{22}^{(k)} \end{bmatrix}\right\} \quad (14)$$

(Jacobian matrix and its inverse for the k^{th} iteration)

where

$J_{11}^{(k)} = |V_2|^{(k)}|V_1||Y_{21}|\sin[(\theta_{21}+\delta_1) - \delta_2^{(k)}]$; (15)

$J_{12}^{(k)} = |V_1||Y_{21}|\cos[(\theta_{21}+\delta_1) - \delta_2^{(k)}] + 2|V_2|^{(k)}|Y_{22}|\cos\theta_{22}$; (16)

$J_{21}^{(k)} = |V_2|^{(k)}|V_1||Y_{21}|\sin[(\theta_{21}+\delta_1) - \delta_2^{(k)}]$; (17)

$J_{22}^{(k)} = -|V_1||Y_{21}|\sin[(\theta_{21}+\delta_1) - \delta_2^{(k)}] - 2|V_2|^{(k)}|Y_{22}|\sin\theta_{22}$; (18)

$$\begin{bmatrix} \Delta\delta_2^{(k)} \\ \Delta|V_2|^{(k)} \end{bmatrix} = inv\{J^{(k)}\}\begin{bmatrix} \Delta P_2^{(k)} \\ \Delta Q_2^{(k)} \end{bmatrix} \quad (19)$$

$|V_2|^{(k+1)} = |V_2|^{(k)} + \Delta|V_2|^{(k)}$; (new value of $|V_2|$ at the end of the k^{th} iteration) (20)

$\delta_2^{(k+1)} = \delta_2^{(k)} + \Delta\delta_2^{(k)}$; (new value of δ_2 at the end the k^{th} iteration) (21)

The final and required values of $|V_2|$ and δ_2 are obtainable from eqn. (20) and (21).

Concerning the maximum power deliverable (P_{2max}) and the line maximum reactive power capability (Q_{2max}), the relevant load flow equations are obtained from the phasor diagram of Fig. 2(d) as follows:

$|V_1|^2 = (|V_2|+|V_x|)^2 + |V_y|^2$

$= (|V_2| + R|I_m|\cos\phi_m + X|I_m|\sin\phi_m)^2 + (X|I_m|\cos\phi_m - R|I_m|\sin\phi_m)^2$

$= (|V_2| + [RP_2 + XQ_2]/|V_2|)^2 + ([XP_2 - RQ_2]/|V_2|)^2$ (22)

Expanding and simplifying this yields the quadratic equations in terms of ($|V_1|^2$) which are

$(|V_2|^2)^2 + [2(RP_2 + XQ_2) - |V_1|^2](|V_2|^2) + (R^2 + X^2)(P_2^2 + Q_2^2) = 0$ (23)

Substituting for $Z^2 = (R^2 + X^2)$; $Q_2 = P_2(1+\tan\phi_m)$ in eqn. (23) gives

$(|V_2|^2)^2 + [2P_2(R+ X\tan\phi_m) - |V_1|^2](|V_2|^2) + P_2^2Z^2(1+\tan^2\phi_m) = 0$ (24)

Also, substituting for $Z^2 = (R^2 + X^2)$; $P_2 = Q_2/(1+\tan\phi_m)$ in the same eqn. (27) yields

$\tan^2\phi_m(|V_2|^2)^2 + [2Q_2\tan\phi_m(R + X\tan\phi_m) - |V_1|^2\tan^2\phi_m](|V_2|^2) + Q_2^2Z^2(1+\tan^2\phi_m) = 0$ (25)

The quadratic equations (24) and (25) obviously have the solution of the form

$|V_2| = [-(b/2a) \pm [(b/2a)^2 - (c/a)]^{½}]^{½}$ (26)

Now, as a function of the load bus active power, P_2, one voltage solution can be written as

$|V_2| = \text{sqrt}\{[(|V_1|^2/2) - P_2(R+ X\tan\phi_m)] + \text{sqrt}\{[P_2(R+ X\tan\phi_m) - (|V_1|^2/2)]^2 - [P_2^2Z^2/(\cos^2\phi_m)]\}\}$ (27)

Also, as a function of the load bus reactive power, Q_2, another voltage solution can be written as

$|V_2| = \text{sqrt}\{[(|V_1|^2/2) - Q_2(R+ X\tan\phi_m)\cot\phi_m]$
$+ \text{sqrt}\{[Q_2(R+ X\tan\phi_m)\cot\phi_m - (|V_1|^2/2)]^2 - [Q_2^2Z^2/(\sin^2\phi_m)]\}\}$ (28)

And from eqn. (27) and (28), two other quadratic equations in terms of P_2 and Q_2 are obtainable, their solutions being expressed as follows:

$P_2 = -[|V_2|^2(B/D) + E] + \text{sqrt}\{[(|V_2|^2B/D)^2 + (2BE/D)|V_2|^2 + E^2] - [|V_2|^2(|V_2|^2 - 2A)/D]\}$ (29a)

where

$A=(|V_1|^2/2)$; $B = (R+ X\tan\phi_m)$; $C = B|V_1|^2$; and $D = Z^2/\cos^2\phi_m$; and $E = (C/2D) - (AB/D)$ (29b)

$Q_2 = -[|V_2|^2(B'/D') + E'] +$
$\text{sqrt}\{[(|V_2|^2B'/D')^2 + (2B'E'/D')|V_2|^2 + E'^2] - [|V_2|^2(|V_2|^2 - 2A')/D']\}$ (30a)

where

$A'=(|V_1|^2/2)$; $B' = (R+ X\tan\phi_m)\cot\phi_m$; $C' = B'|V_1|^2$; and $D' = Z^2/\sin^2\phi_m$
$D' = Z^2/\sin^2\phi_m$; and $E' = (C'/2D') - (A'B'/D')$ (30b)

Equations 29(a) and 30(a) are used to plot the graphs of Power Delivered v/s Load Bus Voltage. All computations and graph plotting were carried out using MATLAB version R2018a.

2.3 Specifications for Load-Flow Computations

$S_2 = -[0.314 + j0.13]$ p.u.= $-0.34/\underline{22.5^o}$; (complex load power) (31)

$P_2^{(sch)} = -0.314$ p.u.; $Q_2^{(sch)} = -0.13$ p.u.; (scheduled power components) (32)

$|V_1| = 1.0$ p.u.; $|V_2|^{(0)} = 1.0$ p.u.; (initial input and output voltage values) (33)

$\delta_1 = 0.0$ rad.; $\delta_2^{(0)}$ rad.= 0.0; (initial input and output load angle values) (34)

$Z = 0.0578+j0.2024 = 0.2105/\underline{74.1^o}$ p.u. (line impedance) (35)

$y_{12} = y_{21} = 1/Z = 4.75/\underline{-74.1^o}$ or [1.3015–j4.5688] p.u. (line series admittance) (36)

$y_{10} = y_{20} = 1/X_{10} = 0.078\underline{/+90^o}$ or [0 + j0.078] p.u. (line charging shunt admittances) (37)

2.4) MATLAB Return of Load-Flow Computations for V_2 and δ_2

As in [10] MATLAB returned the data presented here when the above specified variables were duly applied.

NEWTON-RAPHSON LOAD FLOW ANALYSIS OF BENIN-IRRUA 132KV LINE
The Load Bus Admittance Matrix
1.3015 - 4.4908i -1.3015 + 4.5688i
-1.3015 + 4.5688i 1.3015 - 4.4908i

FIRST ITERATION
Enter value of specified bus voltage, V2_it:1
Enter value of specified bus angle, d2_it:0

The System Jacobian Matrix
4.5688 1.3070
-1.3014 4.4112

Column Vector giving Change in Bus Angle (d2_ch), and
Change in Bus Voltage Magnitude (V2_ch), respectively.
-0.0609
-0.0296

Enter value of change in bus angle (d2_ch):-0.0609
Enter value of change in bus voltage: (V2_ch)-0.0296

Resultant Load Bus Voltage Magnitude (p.u.):
0.9704

Resultant Load Bus Angle Value (radian):
-0.0609

SECOND ITERATION
Enter value of specified bus voltage, V2_it:0.9704
Enter value of specified bus angle, d2_it:-0.0609

Column Vector giving Change in Bus Angle (d2_ch), and
Change in Bus Voltage Magnitude (V2_ch), respectively.
-0.0020
-0.0030

Enter value of change in bus angle (d2_ch):-0.0020
Enter value of change in bus voltage (V2_ch):-0.0030
Resultant Load Bus Voltage Magnitude (p.u.):
0.9674

Resultant Load Bus Angle Value (radian):
-0.0629

FUTHER ITERATION
Enter value of specified bus voltage, V2_it:0.9674
Enter value of specified bus angle, d2_it:-0.0629

Column Vector giving Change in Bus Angle (d2_ch), and
Change in Bus Voltage Magnitude (V2_ch), respectively.
1.0e-004 *
-0.4849
-0.2638

Clearly from the above, $V_2 = 0.9674$ p.u., $\delta_2 = -0.0629$ rad. or 3.6 deg.

 ISSN: 2645-2685

2.5 MATLAB Return of Load-Flow Computations for P_{2max} and Q_{2max}

Also, in [10] it is given that MATLAB returned the following in respect of P_{2max} and Q_{2max} using the data earlier specified above.

**FINDING THE POINT OF MAXIMUM LOADABILITY (PML)AND
THE MAXIMUM REACTIVE POWER DELIVERABLE (ALL IN P.U.)**

Enter Value of Load PF Angle Selected (in radian), G:0.3927

G =

0.3927

Point of Maximum Loadability, PML, (p.u.) with Lagging PF Load
1.3533

Maximum Active Power (MW) Deliverable with Lagging PF Load
135.3250

Maximum Reactive Power (MVAr) Deliverable with Lagging PF Load
56.0

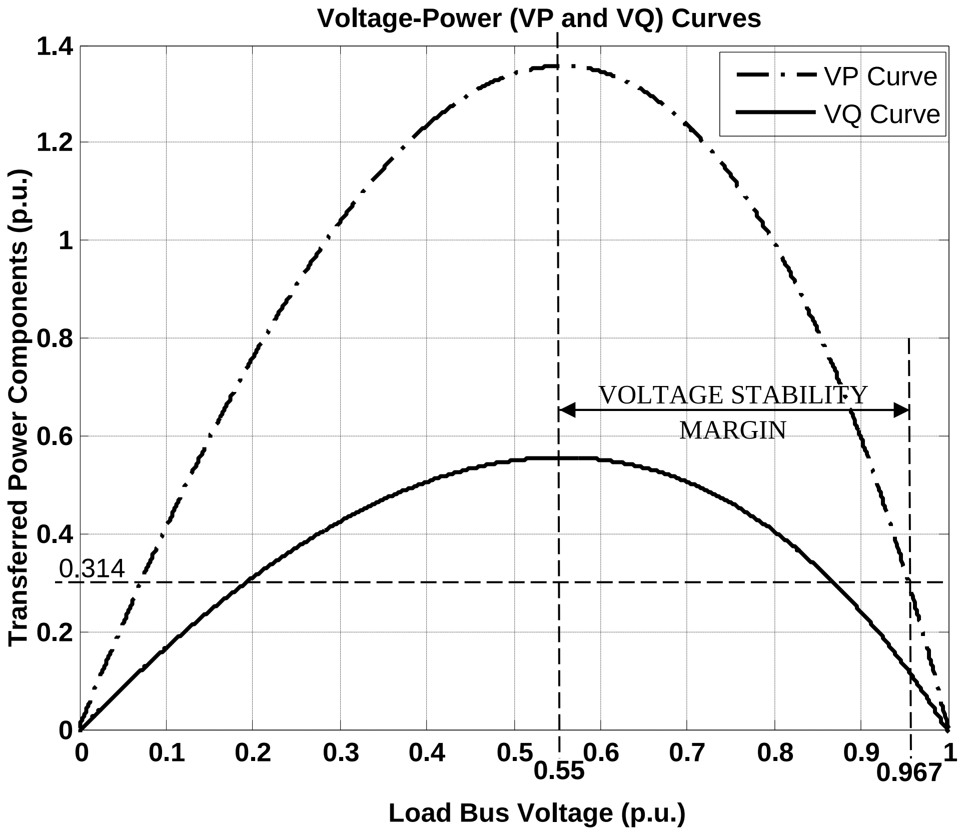

Fig. 3: VP and VQ Curves for PML and Maximum MVAr Determination
(being a MATLAB Plot from the Relevant Load Flow Equations)

Obviously, P_{2max} = 135MW (1.35 p.u.) and Q_{2max} = 56MVAr (0.56 p.u.)

2.6 Various Stability Assessment Indices

As drawn from [5, 6, 15] the stability assessment indices considered here include Nos. 1) to 6) which are based on load/system impedance method, and Nos. 7) to 10) which are based on system maximum-loadability method.

1) *Voltage Stability Load Bus Index (VSLBI):*

$$VSLBI = V_2/\Delta V_{ZTH} \quad (8)$$

Generally,

$$I_{12} = y_{12}(V_1 - V_2) + V_1 y_{10}; \text{ and } \Delta I_{12} = y_{12}(\Delta V_1 - \Delta V_2) + \Delta V_1 y_{10} \quad (9)$$

Since,

$$\Delta V_1 = 0 \ \ then \ \ \Delta I_{12} = -y_{12}(\Delta V_2) \ where \ \Delta V_2 = 0.9674 - 1.0 = -0.0326 \, p.u. \quad (10)$$

And,

$$\Delta V_{ZTH} = -y_{12}(\Delta V_2) * Z_{TH} = -(\Delta V_2); because \ \ y_{12} Z_{TH} = 1 \quad (11)$$

Thus,

$$\Delta V_{ZTH} = -(-0.0326) = 0.0326 \, p.u.$$

So,

$$\boldsymbol{VSLBI} = \frac{0.9674}{0.0326} = \mathbf{29.67 \, p.u.}$$

2) *Impedance Stability Index (ISI):*

$$ISI = \frac{Z_{sys}}{Z_{load}} = \frac{Z_{TH}}{Z_{load}} = \frac{Z_{12}}{Z_{load}} \quad (12)$$

$$\boldsymbol{ISI} = \frac{0.2105}{2.845} = \mathbf{0.074 \, p.u.}$$

3) *Fast Voltage Stability Index (FVSI):*

$$\boldsymbol{FVSI} = 4\left[\frac{Z_{TH}^2 \, Q_2}{V_1^2 \, X_{12}}\right] \quad (13)$$

$$= 4\left[\frac{0.2105^2 * 0.13}{1.0 * 0.2024}\right] = \mathbf{0.1138 \, p.u.}$$

4) *Voltage Index Predictor (VIP):*

$$\text{VIP} = \frac{(V_2 - Z_{TH} I_{12})^2}{4 Z_{TH}} = \Delta S \ (change \ in \ complex \ power) \quad (14)$$

$$I_{12} = 4.7506 * (1.0 - 0.9674) + 1.0 * 0.078 = 0.2329$$

i.e. $$\boldsymbol{VIP} = \frac{(0.9674 - [0.2105 * 0.2329])^2}{4 * 0.2105} = \mathbf{1.00 \, p.u.}$$

5) *Transmission Path Stability Index (TPSI):*

$$TPSI = 0.5V_1 - (V_1 - V_2 cos\delta_2) = V_2 cos\delta_2 - 0.5V_1 \quad (15)$$

i.e. $$\boldsymbol{TPSI} = V_2 cos\delta_2 - 0.5V_1 = (0.9674 * cos3.6) - (0.5 * 1.00) = \mathbf{0.4655 \, p.u.}$$

6) *Line Stability Index (Lmn):*

$$\boldsymbol{Lmn} = 4\left[\frac{X_{12} Q_2}{V_1^2 \, sin^2(\theta - \delta)}\right] \quad (16)$$

$$= 4\left[\frac{0.2024 * 0.13}{1.0 * sin^2(74.1 - 3.6)}\right] = \mathbf{0.1184 \, p.u.}$$

7) *Voltage Stability Index (VSI):*

$$\text{VSI} = \left[\frac{(P_{2max} - P_2)}{P_{2max}} * \frac{(Q_{2max} - Q_2)}{Q_{2max}} * \frac{(S_{2max} - S_2)}{S_{2max}}\right] \quad (17)$$

where $$S_{2max} = \frac{V_1^2 |[Z_{TH} - (Xsin\emptyset + Rcos\emptyset|]}{2(Xcos\emptyset - Rsin\emptyset)^2} \quad (18)$$

$$= \frac{1[0.2105 - (0.2024 \, sin22.5 + 0.0578 \, cos22.5]}{2(0.2024 \, cos22.5 - 0.0578 \, sin22.5)^2} = 1.465$$

i.e. $$\textbf{VSI} = \left[\frac{(1.35 - 0.314)}{1.35} * \frac{(0.56 - 0.13)}{0.56} * \frac{(1.465 - 0.34)}{1.465}\right]$$

$$= 0.7674 * 0.7679 * 0.7679 = \mathbf{0.4525 \, p.u.}$$

8) *Power Transfer Stability Index (PTSI):*

$$PTSI = \frac{2 S_{load} Z_{TH} (1 + \cos(\theta - \emptyset))}{V_1^2} \quad (19)$$

$$S_{load} = 0.314 + j0.13 = 0.34\angle(22.5) \text{ deg}; \ Z_{TH} = Z_{12} = 0.2105\angle(74.1) \text{ deg}$$

$$Z_{load} = \frac{|V_1^2|}{S_{load}^*} = \frac{|V_1^2|}{P_2 - jQ_2} = 2.845\angle(22.5) \text{ deg}; \ \emptyset = 22.5 \text{ deg}; \ \theta = 74.1 \text{ deg}$$

$$\boldsymbol{PTSI} = \frac{2 * 0.34 * 0.2105(1 + \cos(74.1 - 22.5))}{1.0} = \mathbf{0.232 \, p.u.}$$

9) *Voltage Collapse Potential Indices (VCPI):*

$$VCPI(i) = \frac{P_2}{P_{2max}}; \quad VCPI(ii) = \frac{Q_2}{Q_{2max}} \tag{20}$$

i.e. $$\boldsymbol{VCPI(i)} = \frac{0.314}{1.35} = \mathbf{0.2326\ p.u.}; \quad \boldsymbol{VCPI(ii)} = \frac{0.13}{0.56} = \mathbf{0.2321\ p.u.}$$

10) Voltage Stability Margin (VSM):

From the MATLAB Plot of Fig. 3, the bus voltage for P_{2max}, is V_{2pm} = 0.55x132 = 72.6kV; and bus voltage for P_2 delivered is V_{2pd} = 0.967x132 =127.6kV

$$\boldsymbol{VSM} = \frac{V_{2pd} - V_{2pm}}{V_{2pm}} \tag{21}$$

$$= \frac{127.6 - 72.6}{72.6} = \mathbf{0.7576\ p.u.}$$

3. RESULTS AND DISCUSSION

The results of the computations are provided in Table 1 that immediately follows. The table also provides standard specifications concerning the stability indices.

Table 1: Computed Stability Index Values and their Standard Specifications

S/ No.	Indices	Value Obtained (as X p.u.)	Standard Specifications		Method
			Stable State (X p.u.)	State of Collapse (X p.u.)	
1	VSLBI	29.67	X > 1	X = 1	Load/System Impedance Method
2	ISI	0.074	0 ≤ X < 1	X = 1	
3	FVSI	0.1138	0 ≤ X < 1	X = 1	
4	VIP	1.00	0 < X ≤ 1	X = 0	
5	TPSI	0.4655	0 < X ≤ 1	X = 0	
6	Lmn	0.1184	0 ≤ X < 1	X = 1	
7	VSI	0.4525	0 < X ≤ 1	X = 0	System Maximum Loadability Method
8	PTSI	0.232	0 ≤ X < 1	X = 1	
9	VCPI(i)	0.2326	0 ≤ X < 1	X = 1	
	VCPI(ii)	0.2321	0 ≤ X < 1	X = 1	
10	VSM	0.7576	0 < X ≤ 1	X = 0	

The letter "X" is used generally in the table to stand for index value (whether that obtained by computation or that of standard specification). The standard specifications as given in the 4th and 5th columns of the above Table are as provided in [5, 6, 9, 16, 17, 18, 19, 20]. It can be seen that only two of the ten indices, namely, VSI and TPSI, give indication close to a 50/50% chance of stable and collapsed conditions; which is okay. The indices FVSI, Lmn, PTSI, VCPI and VSM (five of them) provide indication to very good static voltage stability condition; whereas, the remaining three ISI, VIP and VSLBI are pointers to excellent static voltage stability condition.

4. CONCLUSION AND RECOMMENDATION

Going by the values of the indices as obtained from computations, and as provided in Table 1, the Benin-Irrua medium transmission line (MTL) is a very stable line in terms of voltage profile, and by extension, as far as loadability is concerned. This is, of course, recommendable for adoption in the construction of any future 132 KV lines in the country, or where an existing 132 KV line has to be reconstructed.

REFERENCES

[1] El-Saadawi M. M. (2005): Electrical Power System – Characteristics and Performance of Transmission Lines; Course Code: FCR 141; www.saadawi.net/uploadedFiles/extra_files/9181non8nj_pdf. (04/05/2017).

[2] Tcheslavski G. V. (2008): Lecture 9 – Transmission Lines; Fundamentals of Power Engineering; ELEN 3441. https://doctord.dyn.org/Course/.../Lecture%2009%20-%20Transmission%20lines.pdf (04/05/2017)

[3] Parsai N. & Thakur A. (2015): PV Curve-Approach for Voltage Stability Analysis; *International Journal of Scientific Research Engineering & Technology (IJSRET)*; Vol. 4, Issue 4; pp.373 – 377.

[4] Johnson S. (1998): Long-term Voltage Stability in Power Systems; PhD Thesis, Department of Electric Power Engineering; Chalmers University of Technology; Goteborg, Sweden; Technical Report No. 335.

[5] Reis C. & Barbosa F. P. M. (2006): A Comparison of Voltage Stability Indices; *IEEE MELECON*; Benalmadena (Malaga), Spain; pp. 1007 – 1010.

[6] Storvann V. (2002): Maintaining Voltage Stability – An Analysis of Voltage Stability and Mitigating Actions; M. Sc. Thesis, Department of Electric Power Engineering; Norwegian University of Science and Technology; NTNU – Trondhein.

[7] Sauer P. W. (2003): What is Reactive Power?; Power Systems Engineering Research Centre; 428 Phillips Hall, Cornell University, Ithaca.

[8] Bhaladhare S. B., Telang A. S. & Bedekar P. P. (2013): P-V, Q-V Curve – A New Approach for Voltage Stability; National Conference on Innovative Paradigms in Engineering & Technology; *Proceedings published by International Journal of Computer Applications & IJCA.*

[9] Adebayo I., & Sun Y. (2017): New Performance Indices for Voltage Stability Analysis in a Power System; Energies – MPDI, 10, 2042; 103390/en10122042; www.mdpi.com/journal/energies 25/09/2016

[10] Enyong P. M. (2018): Determination of the Line Losses and Loadability Limits of the Benin-Irrua 132 KV Transmission Line; *Proceedings of International Conference on Research and Innovation in Engineering*; Vol. 1, No. 2, December 3 – 6; Faculty of Engineering, University of Uyo, Nigeria; pp. 66 –75.

[11] Chary D, V, M., Subramanyam M. V. & Kishor P. (2017): PV Curve Method for Voltage Stability and Power Margin Studies; *International Journal of Engineering and Computing*; Vol. 7, No. 5; pp. 11867–11869.

[12] Mehta V. K. and Mehta Rohit (2009): *Principles of Electrical Machines*, 2nd Ed., New Delhi, S. Chand & Company Limited.

[13] Shepherd J. Morton A. H. & Spence L. F. (1970): *Higher Electrical Engineering*, 2nd Ed., London, Pitman Publishing Limited; pp.248-258

[14] Halder-Dey S., Nagendra P. & Paul S. (2016): Global Voltage Stability Analysis of a Power System using Network Equivalencing Technique in the Presence of TCSC; https://lejpt.academicdirect.org/A16/get_htm.php? (02/07/2018)

[15] Ramirez-Perodomo S. L. & Lozano C. A. (2014): Evaluation of Indices for Voltage Stability Monitoring using PMU Measurements; Ingenieria e Investigacion, 34(3), 44 – 49.

[16] Rui Sun (2009): Voltage Stability Indices Based on Active Power Transfer using Synchronized Phasor Measurements; M. Eng. (Power System) Thesis of the Clemson University.

[17] Tran M. T. (2009): Definition and Implementation of Voltage Stability Indices in PSS®NETOMAC; M. Eng. (Electric Power Engineering) of Chalmers University of Technology; Sweden.

[18] Eleschova Z. & Belan A. (2008): The Power System Steady-State Stability Analysis; AT & P Journal PLUS 2; pp. 54–57.

[19] Telang A. S. & Bedekar P. P. (2016): Application of Voltage Stability Indices for Proper Placement of STATCOM under Load Increase Scenario; *International Journal of Energy and Power Engineering*; World Academy of Science, Engineering and Technology; Vol. 10, No. 7; pp. 998 – 1003.

[20] Neerugattu L. & Raju G. S. (2012): New Criteria for Voltage Stability Evaluation in Interconnected Power System; VNR Vignana Jyothi Institute of Engineering & Technology, Bachupally, Hyderabad; pp. 1 – 6.